Is the mid-diastolic isthmus always the best ablation target for re-entrant atrial tachycardias?

Is always the mid-diastolic isthmus the best ablation target for re-entrant atrial tachycardias?

SHORT TITLE: Re-entrant atrial tachycardias ablation: new insights from ultra-high density mapping

Antonio De Simone, MD (1); Matteo Anselmino, MD (2); Marco Scaglione, MD (3); Giuseppe Stabile, MD (4); Francesco Solimene, MD (5); Antonio De Bellis, MD (1); Marco Pepe, MD (1); Alfonso Panella, MD (1); Federico Ferraris, MD (2); Maurizio Malacrida, BS (6); Francesco Maddaluno, BS (6); Fiorenzo Gaita, MD (2); Ignacio García-Bolao, MD (7).

From: 1 Clinica San Michele, Maddaloni (CE), Italy; 2 "Città della Salute e della Scienza di Torino" Hospital, Department of Medical Sciences, University of Turin, Italy; 3 Cardinal Massaia Hospital, Asti, Italy; 4 Clinica Mediterranea, Naples, Italy; 5 Clinica Montevergine, Mercogliano (AV), Italy; 6 Boston Scientific Italia, Milan, Italy; 7 Clinica Universidad de Navarra, Pamplona, Spain.

Address for Correspondence

Antonio De Simone

Laboratorio di Elettrofisiologia, Clinica San Michele,

Via Montella, 16, Maddaloni (CE) 81024, Italy

TEL +39 0823 208818;

FAX +39 0823 208818;

e-mail elettrofisiologiasanmichele@gmail.com

ORCID

Antonio De Simone 0000-0002-3864-0375

Word Count: 3331

Conflicts of Interest

Maurizio Malacrida and Francesco Maddaluno are employees of Boston Scientific; no other conflicts of interest exist.

KEYWORDS: catheter ablation; high-density mapping; Intra-atrial re-entrant tachycardia; mid-diastolic activity

ABSTRACT

Aims: We evaluated the ability of an ultra-high mapping system to identify the most convenient ablation target (RAT) in intra-atrial re-entrant tachycardias (IART) in terms of the narrowest area to transect in order to interrupt the re-entry.

Methods: 24 consecutive patients were enrolled with a total of 26 IARTs. The Rhythmia mapping system was used to identify the RAT in all IARTs.

Results: In 18 cases the RAT matched the mid-diastolic phase of the re-entry whereas in 8 cases the RAT differed. In these patients, the mid-diastolic tissue in the active circuit never represented the area with the slowest conduction velocity (CV) of the re-entry. The mean CV at the mid-diastolic site was significantly slower in the group of patients in which the RAT matched the mid-diastolic site (p=0.0173) and that of the remaining circuit was significantly slower in the group in which the RAT did not match (p=0.0068). The mean CV at the RAT was comparable between the two group (p=0.66).

Conclusions: Identifying the RAT in challenging IARTs by means of high-density representation of the wave-front propagation of the tachycardia seems feasible and effective. In one-third of cases this approach identifies an area that differs from the mid-diastolic corridor.

INTRODUCTION

Intra-atrial re-entrant tachycardias (IART) arising after atrial fibrillation (AF) ablation or surgical intervention constitute a diagnostic and therapeutic challenge. IART are sustained by the presence of a critical isthmus of conductive myocardial tissue through which the wave-front of depolarization propagates, perpetuating the tachycardia. However, the main difficulties in treating IART are due to the common coexistence of multiple re-entrant loops and the presence of complex atrial substrates, such as areas of scarring.

Catheter ablation is considered to be the only curative treatment for this kind of arrhythmia. The goal of the transcatheter procedure is to identify the narrowest conduction isthmus within the circuit and eliminate it by means of ablation in the most specific and safe manner. Previous studies [1-6] have suggested that the ideal ablation site is the diastolic pathway of the tachycardia, an area of slow conduction where mid-diastolic electrograms (EGM)s are recorded. In the light of this evidence, it is common practice to approach IARTs[6] by establishing a specific window of interest (WOI), based on ECG atrial activation wavers, to identify the mid-diastolic isthmus on the endocardial electroanatomic activation map.

The Rhythmia mapping system (Boston Scientific, Inc, Cambridge, MA) is a new high-density mapping system that enables wave-front propagation to be identified with a previously unattainable level of detail and resolution [7] . The present pilot study evaluates feasibility and efficacy of this system to identify the most appropriate ablation target – the narrowest area to transect in order to interrupt the re-entry - exclusively on the basis of detailed analysis of conduction velocity of the wave-front propagation,

METHODS

Study population. From January 2016 to December 2016, 24 consecutive patients from 3 Italian and 1 Spanish centers were enrolled. The inclusion criterion was the presence of persistent IART after previous catheter ablation for AF or after a surgical procedure involving incision of the atria. Inclusion of the patients in each local AF registry was approved by the local Institutional Review Board. The study complies with the Declaration of Helsinki. All patients provided written informed consent.

Standard Electroanatomic mapping. EGMs in the right atrium (RA) and/or the left atrium (LA) were collected by means of a 64-pole mini-basket mapping catheter (IntellaMap Orion, Boston Scientific, Inc, Cambridge, MA). Two reference EGMs (one main [R] and one additional [ΔR]) were chosen on the decapolar catheter, which was placed in the coronary sinus (CS). Heartbeats were automatically selected for inclusion in the map on the basis of cycle length (CL) stability, stable relative timing of the 2 reference EGMs, electrode location stability, and respiratory gating. To annotate the local activation time of each acquired bipolar EGM, the system combines unipolar (maximum negative dV/dt) and bipolar (maximum amplitude) EGMs. In the case of fragmented or multiple potential EGMs, the system takes into account the timing in the surrounding area, in order to select the potential to use for timing annotation. The scar setting can be finely tuned by means of the confidence mask tool (points in the immediately surrounding area that have an EGM bipolar amplitude below the confidence mask have no color code and are displayed in gray) even far below the current scar cutoff of classically available systems (< 0.1 mV). Being exposed to a low signal averaging and cancellation effects, the small, closely-spaced, low-noise electrodes of the Orion catheter provide greater mapping resolution, potentially identifying low and fractionated potentials of surviving bundles in a presumed dense scar or in a previously ablated area [8-10].

In order to identify the mid-diastolic corridor in the activation map, we calculated the backward and forward intervals of the WOI according to the following formulas:

$$Backward\ \ interval = \frac{TCL - DUR^{PW}}{2} + Interval^{PWonset-ref}$$

$$Forward\ Interval = (TCL - Backward\ Interval)\ x\ 1$$

where TCL is the tachycardia cycle length duration, DUR^{PW} is the duration of the surface P wave on the 12 lead surface ECG during IART and $Interval^{PWonset-ref}$ is the interval between the onset of the P wave and the reference signal, which has a negative value when the reference signal precedes the P wave. In the original formula [6], the multiplying factor used to calculate the forward interval was 0.90/0.95, because the WOI duration spanned from 90% to 95% of the TCL. Considering that the WOI duration is designed to span the entire CL duration, on using the

Rhythmia software, we adopted a multiplying factor of 1 in our calculation of the forward interval. With this setting, red and orange on the color-coded activation map identify mid- and late-diastolic activations, respectively, and dark blue and purple identify early- and mid-diastolic activations, respectively. The remaining colors identify areas of systolic activation. The area of "early-meets-late" is the interface between the red area and the purple area, and identifies the mid-diastolic corridor of the re-entry circuit.

Rhythmia specific propagation mapping. For each IART, the wave-front propagation was visualized dynamically, following a short (20ms) time-window of activation (displayed as a dark red front), which was slowly advanced manually along the timescale. Sites of narrowing of the wave-front were indicative of slowing of conduction in that area. Thus, the activated area was rather broad in normal (fast) conduction velocity (CV) regions; it then became narrow when CV decreased, and widened again when CV increased (Fig. 1).

CV was subsequently measured offline by dividing the distance between successively activated points (in the direction of the main wave-front propagation) by the time (the difference between the times of local activation of 2 points situated in areas of visually homogenous CV). [11-13] If the CV along a specific area was not homogeneous, according to the propagation map analysis, the CV of each homogeneous area was calculated and then the final CV of the site was calculated as the algebraic mean of the calculated CVs. CV was also calculated in the areas emerged at interest following visualization of the narrowing of the dynamic wave-front propagation, and, in addition, in the following segments: roof, septum, anterior wall, posterior wall and lateral wall of the LA, and cavo-tricuspid istmus (CTI), lateral wall, septum, anterior wall and posterior wall of the RA.

Rhythmia ablation target. Analysis of Rhythmia specific propagation map was the only means used in this study to select the ideal ablation target for each IART. Dynamic analysis of the wave-front propagation of the re-entry allows identification of anatomical barriers, areas of scarring, lines of block, bystander areas and active tissue through which the depolarization wave-front must propagate in order to perpetuate the tachycardia. On the basis of a thorough analysis of the wave-front propagation, and relative CVs, we defined the Rhythmia ablation target (RAT) of each IART as the narrowest area of slow conduction to transect in order to interrupt the re-entry circuit. Entrainment[6] was used to validate the isthmus identified by electroanatomic mapping as the critical area of re-entry at physician's discretion. In re-entry circuit sites when it was difficult to evaluate surface electrocardiogram or an intracardiac electrogram at the mapping

site the N + 1 difference technique was used.[14] Examples of entrainment maneuvers are reported as Supplementary Materials (Supp. Fig.1, Supp. Fig. 2).

Ablation. Ablation was performed at the RAT. Even in case of early IART termination during RF applications, ablation was always continued in order to create a line of bidirectional block connecting neighboring areas of block/scar. The procedure was considered successful if the IART terminated during RF ablation and could not be re-induced via multiple extra-stimuli and bursts 30 minutes after the termination of ablation. If a new inducible morphology of IART with stable TCL emerged, the new arrhythmia was further mapped and targeted for ablation. Additional ablations were also performed in the event of pulmonary vein re-connection documentation to eliminate potential arrhythmia triggers. Ablation was performed by means of an irrigated-tip ablation catheter (IntellaNAV OI, Boston Scientific, Inc, Cambridge, MA, or Thermocool, Biosense-Webster Inc., Diamond Barr, CA, USA) with a maximum power set to 40 W. The flow rate was set at 17 mL/min for power settings under 30 W and at 30 ml/min for power settings above 30 W.

Clinical management. Oral anticoagulation was continued on the day of the procedure and was subsequently administered for at least 3 months (*ad vitam* in patients with a CHA2DS2-VASC score ≥2). Antiarrhythmic drugs were usually discontinued ≥5 half-lives prior to ablation, except for amiodarone. Patients were discharged without antiarrhythmic drugs. Patients were scheduled for routine follow-up examinations at least twice a year after the initial treatment, and rhythm monitoring during the follow-up visits was performed through clinical assessment of atrial arrhythmia recurrence, ECG, and 24-hours Holter monitoring.

At follow-up the procedure was deemed successful in the absence of symptomatic or asymptomatic atrial tachy-arrhythmias lasting more than 30 seconds identified on surface ECG or on Holter monitoring, off antiarrhythmic drug therapy. If any recurring symptomatic IART was documented, the patient was offered a second procedure.

RESULTS

Baseline Patient Characteristics. Twenty-four patients were included in the analysis, 13 were male and the mean age was 54 ± 9 years. The majority of the patients (79%) had already undergone at least one catheter ablation procedure (prior AF ablation), whereas 2 patients had developed IART during a pulmonary vein isolation procedure, and 3 had undergone previous surgical procedures.

IART Characteristics. 26 IART were registered in 24 patients. A mean of 19.023±11.197 EGMs for each map were acquired during a mean mapping time of 25 ± 11 minutes. The arrhythmias were: 14 single-loop re-entries in the left atrium, 9 double-loop re-entries, 1 triple-loop re-entry, and 2 atypical right flutters (in patients with scarring at the posterolateral RA site [15-17]. Three patients had more than one IART, including one clinical arrhythmia (documented prior to the procedure) and several additional tachycardias induced by atrial pacing but not documented before the procedure. The most common single-loop IARTs were perimitral (9 out of 14) and roof-dependent flutters (3 out of 14); less commonly the tachycardias were sustained by anterior (1 out of 14) and posterior re-entries (1 out of 14). In 3 cases of single-loop perimitral flutter, baseline endocardial block of the mitral isthmus (documented by the absence of electrical activity or by the presence of clearly distinct double atrial EGMs) was present, and the arrhythmia was sustained by a circuit bridging the epicardial portion of the myocardium (confirmed by CS activation).

Standard and Rhythmia specific mapping. In all IARTs, surface P-wave morphology was clearly identifiable and the previously defined WOI could be correctly set. According to the setting, the interface between red and purple colors in the static activation map identified activated tissue in the mid-diastole timing of the circuit.

In 18 cases (69%) the RAT matched the mid-diastolic site of the re-entry (Tab. 1). In this group of patients, only one clear mid-diastolic site (area where red meets purple) was visible and it always presented the slowest CV of the circuit.

In the remaining 8 cases (31%) the RAT did not match the mid-diastolic site (Tab. 2). In these patients, the mid-diastolic area in the active circuit was not that with the slowest CV (Fig. 2). In addition, in 6 (75%) of these cases, more than one site was activated during mid-diastole (at least two areas where red met purple on the activation map; Fig. 3, Supp. Fig. 3).

Among the cases in which the RAT matched with the mid-diastolic site of the re-entry, the mean TCL was 295 ±78 ms; the mean CV at RAT was 0.24 ± 0.05 ms compared to a mean of 0.74 ± 0.2 ms in the remaining circuit ($p<0.0001$). Among the cases in which the RAT and mid-diastolic EGMs did not match, the mean TCL was 274 ± 53 ms; the mean CV at RAT was 0.23 ± 0.05 ms compared to 0.49 ± 0.2 ms in the remaining circuit ($p=0.0007$). In addition, in the latter group, CV at RAT (0.23 ± 0.05 ms) was significantly slower compared to that at the mid-diastolic area (0.3 ± 0.04 ms; $p=0.0102$). Therefore, while the TCL were comparable between the two groups ($p=0.8847$), the mean CV at the mid-diastolic site was significantly slower in the group of patients in which the RAT matched the mid-diastolic

site (p=0.0173) and that of the remaining circuit was significantly slower in the group in which the RAT did not match (p= 0.0068). On the contrary, the mean CV at the RAT was comparable between the two group (p=0.66).

Outcome of ablation. In 25 out of 26 IARTs, ablation was successfully performed at the RAT. In one case, after ablation at the RAT, the tachycardia changed to a different IART (both TCL and CS activation changed) and subsequently degenerated into AF. The median [25^{th} -75^{th}] total RF delivery duration was 120 [32-332] seconds, and the time to IART termination was less than 1 minute of RF application in 11/26 (42%) of the cases. No procedure-related complications were reported.

During a mean follow-up of 18±3 months, 21 patients (87.5%) remained free of atrial arrhythmias. Two patients suffered recurrence of a different IART; in both cases, the tachycardia was of short duration and did not require a repeat ablation. One patient experienced apparent recurrence of the same IART, but declined to repeat the procedure.

DISCUSSION

Main Findings. In this pilot study, we investigate the use of the Rhythmia high-resolution system in detecting the ideal ablation target in challenging IARTs.

The main findings can be summarized as follows:

1) the mid-diastolic area, considered the ablation target by standard mapping, is not always the slowest conducting tissue inside the circuit. In the present experience this was the case in about 3 quarters of times.

2) when a portion of the active circuit whose CV is slower than the CV in the mid-diastolic area is found, the site candidates as an ideal ablation target to interrupt the circuit, although not being in the mid-diastolic phase of the re-entry. In our study, this was the case in about a third of the cases.

Interpretation. Several authors[6, 18-21] have proposed the shortest line connecting two regions of conduction block activated during the mid-diastolic phase of the re-entry as the most convenient target of ablation. Specific settings for establishing the WOI of the electro-anatomic mapping system [6] and specific pacing maneuvers have also been suggested in order to determine the mid-diastolic corridor [18]. In the present study, detailed visualization of the dynamic wave-front propagation of each re-entry enabled us to identify the RAT as the ideal ablation target in terms of the shortest area of slow conduction to ablate in order to interrupt the circuit. Notably, the most convenient ablation target was the mid-diastolic activated tissue only if it was also the area with the slowest CV within the active circuit. By contrast, if some areas of greater CV slowing were present in the circuit, the most convenient ablation target was never

found to be mid-diastolic in activation. The common feature shared by all the cases in this latter group was the presence of at least one area whose CV was slower than the local CV in the mid-diastolic area. In addition, in most of these patients the static activation map showed the presence of more than one area of mid-diastolic activation, which we found to be a pattern correlated with multiple sites of critical CV slowing in the circuit.

Interestingly, in all the macro-re-entrant IART in which the activation map showed more than one mid-diastolic activated area, the RAT never matched with the mid-diastole of the circuit. This finding could be explained by the fact that the presence of more than one area of mid-diastolic activation inside the same circuit is highly suggestive of several areas of diseased conduction and CV slowing; these areas generate complex activations that can lead to the selection of a shorter isthmus to ablate compared to the standard mid-diastolic corridor. This situation is easily exemplified by a single-loop reentry with multiple mid-diastolic sites. In this IART, only one of the mid-diastolic sites is the active diastolic corridor of the tachycardia. The remaining mid-diastolic activated sites are necessarily bystander areas, and are not necessary for the maintenance of the re-entry; indeed, they are passively activated in the mid-diastole of the circuit because the wave-front propagation slows down at more than one site (Fig. 3). The multiple sites of CV slowing generate a complex activation in the chamber, a condition that requires thorough analysis of the wave-front propagation in order to identify the narrowest area to ablate (which is not necessarily mid-diastolic) and successfully interrupt the arrhythmia. Similar considerations can also be extended to cases of IARTs with multiple loops and multiple diastolic sites, in which the activation is expected to be even more complex than in the previous single-loop example.
This interpretation is surely supported by the finding that, in presence of multiple areas of CV slowing and complex propagation patterns, when the RAT was not mid-diastolic, the mean CV of the entire chamber was significantly slower compared to when it was.

On the other hand, if the activation map of the IART showed only one area of mid-diastolic activation, in most of cases this also was the area with the slowest CV. In the remaining cases, the mid-diastolic pathway was an area of critical CV slowing, but there was an even slower activated area (not mid-diastolic in time), which directed to the narrowest area to ablate in order to interrupt the circuit (Fig. 2).

Very recently Takigawa et al. [22] described the precise mechanism of the most common arrhythmias seen following catheter ablation of atrial fibrillation using the Rhythmia mapping system. They used the propagation map to find a "practical" isthmus whose definition was based on anatomic length and tissue characteristics of the most appropriate

and easiest site for ablation within the circuit. They also compared it to the "anatomical" isthmus, a region of tissue conventionally ablated between fixed anatomic obstacles that are predetermined according to the type of reentry. Similarly to our study, they found that high resolution mapping may help in tailoring a more vulnerable and convenient isthmus to ablate in order to interrupt the circuit. However, they did not investigate whether or not the practical or anatomical isthmus were activated in the mid-diastolic phase of the reentry and the role of conduction velocity as a key parameter to identify the most appropriate ablation target. Additionally, our results seem to suggest the existence of an evaluation criteria able to predict when conventional mid-diastolic isthmus is not the narrowest bridge to ablate in order to interrupt the circuit. The ideal ablation site is that obtaining arrhythmia interruption by minimal lesion of tissue. In this sense identifying the anatomical site, according with RAT, where the shortest line of block can be created holds the potential to reduce time to complete the ablation and complications.

As an example, we can use that presented in Figure 3 – a perimitral flutter). In this case we can highlight multiple slow conduction areas, including the mitral isthmus that is activated in the mid-diastolic phase of the circuit. If we approached the arrhythmia with the "classic method", we would have performed an ablation lesions of approximately 34.9 mm. Once achieved conduction block along this line, the arrhythmia surely would have terminated. However, with the approach hereby proposed, a line of block intersecting the RAT was found of only about 12 mm. RF ablation at this site interrupted the flutter after 19 seconds). Therefore, in diseased cardiac tissue with multiple areas of abnormal conduction, we believe more than one area of slow conduction (confirmed active at electroanatomical activation map), in addition to the mid-diastolic activated tissue, are targets of ablation to interrupt the arrhythmia. The choice of the ideal ablation target should, therefore, be based on the shortest line to create a block (geometric concept) rather than of its timing phase (diastolic or systolic) in the circuit. Most of the times the identified site will be mid-diastolic, but one third of the case not.

Practical implications

Our observations may have direct clinical applicability. An effective strategy for identifying the ideal ablation target in order to interrupt a challenging IART should be based on thorough analysis of the dynamic wave-front propagation of the re-entry circuit, rather than exclusively searching the mid-diastolic activated areas on a static activation map. Although the mid-diastolic corridor was the most convenient ablation target to interrupt the re-entry in most patients,

in 30% of the cases, after CV analysis of the dynamic propagation of the circuit, we were able to recognize narrower areas critical for the maintenance of the re-entry.

Limitations. The present analysis has some limitations. First, we included a small number of patients, without any randomization or the presence of a control group. Second, we did not perform systematically entrainment maneuvers, due to the risk of modifying or terminating the clinical tachycardia in the prediction that local capture within these low-voltage areas may have proved challenging [22]. The choice of whether or not to perform entrainment maneuvers to corroborate the data form the electroanatomical map, was left to physician's discretion. Indeed, comparison with the response to entrainment would have improved our understanding of the electrophysiological characteristics in all patients, nevertheless in the cases in which entrainment maneuvers were performed (n=14), the hypothesis was always confirmed. Third, the mean length of follow-up was brief, therefore conclusions concerning long-term success rates are not yet available. Finally, only few patients had an implanted internal loop-recorder. Therefore, some unrecorded asymptomatic episodes may have occurred, and our success rate may have been overestimated."

Conclusions. Identifying the ideal ablation target in challenging IARTs by means of high-density representation of the wave-front CV propagation of the tachycardia seems feasible and effective. In the majority of cases, this approach identifies an area corresponding to the mid-diastolic corridor, though in one third of the cases it differs. In these latter cases, identifying the RAT, commonly directs ablation to narrower areas than those with mid-diastolic activation.

ACKNOWLEDGEMENT

Source of Funding

No extramural funding will be used to support this work. Maurizio Malacrida and Francesco Maddaluno (Boston Scientific Italia) provided expert review of technical information and methods for Rhythmia mapping system and critical revision of the manuscript.

Compliance with ethical standards

Ethical approval: the study protocol was approved, and all procedures were performed in accordance with the local ethics committee.

Informed consent: all patients provided written informed consent before the procedure

Conflict of interest: M. M. and F. M. are employees of Boston Scientific; no other conflicts of interest exist.

REFERENCES

1. Mesas CE, Pappone C, Lang CC, Gugliotta F, Tomita T, Vicedomini G, et al. Left atrial tachycardia after circumferential pulmonary vein ablation for atrial fibrillation: Electroanatomic characterization and treatment. *J Am Coll Cardiol* 2004;44:1071-1079.

2. Kalman JM, VanHare GF, Olgin JE, Saxon LA, Stark SI, Lesh MD. Ablation of 'incisional' reentrant atrial tachycardia complicating surgery for congenital heart disease: Use of entrainment to define a critical isthmus of conduction. *Circulation* 1996;93:502-512.

3. Ouyang F, Ernst S, Vogtmann T, Goya M , Volkmer M, Schaumann A , et al. Characterization of reentrant circuits in left atrial macroreentrant tachycardia: Critical isthmus block can prevent atrial tachycardia recurrence. *Circulation* 2002;105:1934-1942.

4. Triedman JK., Bergau FD, Saul P, Epstein MR, Walsh EP. Efficacy of radiofrequency ablation for control of intraatrial reentrant tachycardia in patients with congenital heart disease. *J Am Coll Cardiol* 1997;30:1032–8.

5. Kalman JM., VanHare GF, Olgin JE, Saxon LA, Stark SI, Lesh MD. Ablation of "incisional" reentrant atrial tachycardia complicating surgery for congenital heart disease. *Circulation* 1996;93:502–12.

6. De Ponti R Verlato R, Bertaglia E, Del Greco M, Fusco A, Bottoni N, et al. Treatment of macro-re-entrant atrial tachycardia based on electroanatomic mapping: identification and ablation of the mid-diastolic isthmus. *Europace* 2007;9: 449-457

7. Decebal GL, Sok-Sithikun B, Viera F,Delassi T, El Jamili M, Al Amoura A, et al. Selection of Critical Isthmus in Scar-Related Atrial Tachycardia Using a New Automated Ultrahigh Resolution Mapping System. Circ Arrhythm Electrophysiol. 2017

8. Anter E, Tschabrunn CM, Contreras-Valdes FM, Li J, Josephson ME. Pulmonary vein isolation using the Rhythmia mapping system: Verification of intracardiac signals using the Orion mini-basket catheter. Heart Rhythm. 2015;12:1927-34.

9. Tanaka Y, Genet M, Chuan Lee L, Martin AJ, Sievers R, Gerstenfeld EP. Utility of high-resolution electroanatomic mapping of the left ventricle using a multispline basket catheter in a swine model of chronic myocardial infarction. Heart Rhythm. 2015;12:144-54.

10. De Simone A, La Rocca V, Solimene F, Maddaluno F, Malacrida M, Stabile G. Cavo-tricuspid isthmus high density mapping. Heart Rhythm case report 2017.

11 Itoh T, Kimura M, Sasaki S,Owada S, Horiuchi D, Sasaki K,et al. High correlation of estimated local conduction velocity with natural logarithm of bipolar electrogram amplitude in the reentry circuit of atrial flutter. *J Cardiovasc Electrophysiol.* 2014;25:387– 394. doi: 10.1111/jce.12329.

12. Yokokawa M, Latchamsetty R, Ghanbari H, Belardi D, Makkar A, Roberts B, et al. Characteristics of atrial tachycardia due to small vs large reentrant circuits after ablation of persistent atrial fibrillation. *Heart Rhythm*. 2013;10:469–476. doi: 10.1016/j.hrthm.2012.12.018.

13. Bun SS, Latcu DG, Delassi T, Jamili ME, Amoura AA, Saoudi N. Ultra-High Definition Mapping of Atrial Arrhythmias. *Circ J.* 2016;80(3):579-86. doi: 10.1253/circj.CJ-16-0016. Epub 2016 Feb 8.

14. Soejima K, Stevenson WG, Maisel WH, Delacretaz E, Brunckhorst CB, Ellison KE et al. The N + 1 difference: a new measure for entrainment mapping. .J Am Coll Cardiol. 2001 Apr;37(5):1386-94.

15. Fujiki A, Nishida K, Sakabe M, Sugao M, Tsuneda T, Mizumaki K et al. Entrainment mapping of dual-loop macroreentry in common atrial flutter: New insights into the atrial flutter circuit. *J Cardiovasc Electrophysiol* 2004;15:679-685.

16. Takigawa M, Denis A, Frontera A, Derval N, Sacher F, Jaïs P et al. Triple-loop reentrant atrial tachycardia originated after pulmonary vein isolation. *J Interv Card Electrophysiol.* 2017 Apr;48(3):367-368. doi: 10.1007/s10840-016-0187-5.

17. Shah D, Jaïs P, Takahashi A, Hocini M, Peng JT, Clementy J, et al. Dual-loop intra-atrial reentry in humans. *Circulation.* 2000 Feb 15;101(6):631-9.

18. Zipes DP, Jalife J. Macroreentrant atrial tachycardias. In: Zipes DP, Jalife J, eds. Cardiac electrophysiology: From cell to bedside. 5th ed. Philadelphia, PA: *Elsevier*; 2009

19. De Ponti R, Marazzi R, Zoli L, Caravati F, Ghiringhelli S, Salerno-Uriarte JA. Electroanatomic mapping and ablation of macroreentrant atrial tachycardia: comparison between successfully and unsuccessfully treated cases, *J Cardiovasc Electrophysiol* 21:155–162, 2010.

20. Triedman JK, Bergau FD, Saul P, Epstein MR, Walsh EP. Efficacy of radiofrequency ablation for control of intraatrial reentrant tachycardia in patients with congenital heart disease. *J Am Coll Cardiol* 1997;30:1032–8.

21. Triedman JK, Saul P, Weindling SN, Walsh EP. Radiofrequency ablation of intra-atrial reentrant tachycardia after surgical palliation of congenital heart disease. *Circulation* 1995;91:707–14.

22. Takigawa M, Derval N, Frontera A, Martin R, Yamashita S, Cheniti Get al. Revisiting anatomic macroreentrant tachycardia after atrial fibrillation ablation using ultrahigh-resolution mapping: Implications for ablation. *Heart Rhythm*. 2018 Mar;15(3):326-333.

23. Luther V, Sikkel M, Bennett N, Guerrero F, Leong K, Qureshi N et al. Visualizing Localized Reentry With Ultra-High Density Mapping in Iatrogenic Atrial Tachycardia: Beware Pseudo-Reentry. Circ Arrhythm Electrophysiol. 2017 Apr;10(4). pii: e004724. doi: 10.1161/CIRCEP.116.004724

TABLE LEGENDS

1 IART in which the RAT was mid-diastolic

2 IART in which the RAT was not mid-diastolic

FIGURE LEGENDS

1 Roof-dependent IART. In the upper panel, the static activation map shows only one area of mid-diastolic activation, which is located around the gap of an incomplete roof line (double black lines). The lower panel shows some frames of the dynamic propagation map: the dark red front represents 20 ms of activation, which is slowly advanced along the timescale. Sites of narrowing of the wavefront are indicative of slow conduction in that area. In A (modified PA view) the front exiting the gap on the roof and moving posterior and toward the septum. In B (PA view) the posterior wall is activated from right to left. As the activated area is rather broad, CV is normal. In C, the fronts coming from the septum and from the posterior left wall join together (LAO view). In D the wavefront narrows because activation slows

down before crossing the gap. In panel E we see that the mid-diastolic activated tissue was the slowest part of the circuit and matched the RAT (gap in the LA roof)

2 Clockwise re-entry around the tricuspid valve in a patient with an incomplete line of block (double black lines) in the lateral wall. In the upper panel, the activation map shows only one area of mid-diastolic activation along the cavo-tricuspid isthmus. This is an area of CV slowing (panel A in the lower part, mean CV= 0.26 m/s), however, a site of even slower CV can be seen along the gap in the anterolateral line of block (B and C in the lower panel, CV= 0.19 m/s). This area was identified as the RAT and ablation at this spot resulted successful despite it clearly was not mid-diastolic in time. In panel D we can see that the EGM at the RAT site is not mid-diastolic

3 Perimitral flutter whose RAT didn't match the mid-diastolic activated tissue. In the upper panel we can see that the activation map of the circuit shows two areas of mid diastolic activation (red meets purple): mitral isthmus and anterior wall. The propagation map showed a circuit around the mitral valve with an obligated passage through the ridge and the anterior septum (white arrows show the active circuit, grey arrows show bystander activated areas and double straight black lines show fixed or functional areas of block). In the lower panel we can see 2 different frames of the propagation map where the CV significantly slowed down relatively to the rest of the circuit. Among these two areas, only the first one is mid-diastolic in timing (mean CV 0.25 m/s) but it represents the longest area to ablate in order to interrupt the circuit. The arrhythmia was interrupted in the area number two (CV 0.21 m/s) by connecting the isolated RSPV to the area of block indicated by the double black lines in the upper panel. In panel 3 we can see that the EGM at the RAT is not mid-diastolic.

Supplementary Figure 1. Good entrainment response from a site in the mid -diastolic phase of the reentry. We can see the entrainment response from an area of the circuit where the electrogram was mid-diastolic in time. Pacing was performed from the ablation catheter at a slightly (20 ms) shorter cycle length compared to the tachycardia cycle length. The return electrogram from the pacing site when pacing was stopped was not clearly seen due to stimulation saturation artifact so we employed the N+1 technique to measure the post pacing interval [14]. The post pacing interval, as the time form the last stimulus that entrained the tachycardia and the second tachycardia beat after this stimulus was similar (within the ± 20 ms range) to twice the tachycardia cycle length, confirming that the pacing site was part of the circuit

Supplementary Figure 2. Good entrainment response from a slow conduction site that was not at the mid -diastolic phase of the reentry. We can see the entrainment maneuver from a site that was not mid diastolic in timing (the local electrogram at the pacing site was just at the terminal portion of the flutter wave).

Supplementary Figure 3. Width of ablation line at RAT (Panel A, left) and at mid-diastolic mitral isthmus (Panel B, right). D represents the straight line connecting the two white measuring circles (12.1 mm at the RAT and 32.5 mm at the mid-diastole) while L represents the same distance calculated as a curvilinear line along the map surface (12.4 mm at RAT and 34.9 mm at mid-diastole)

Figure 1.

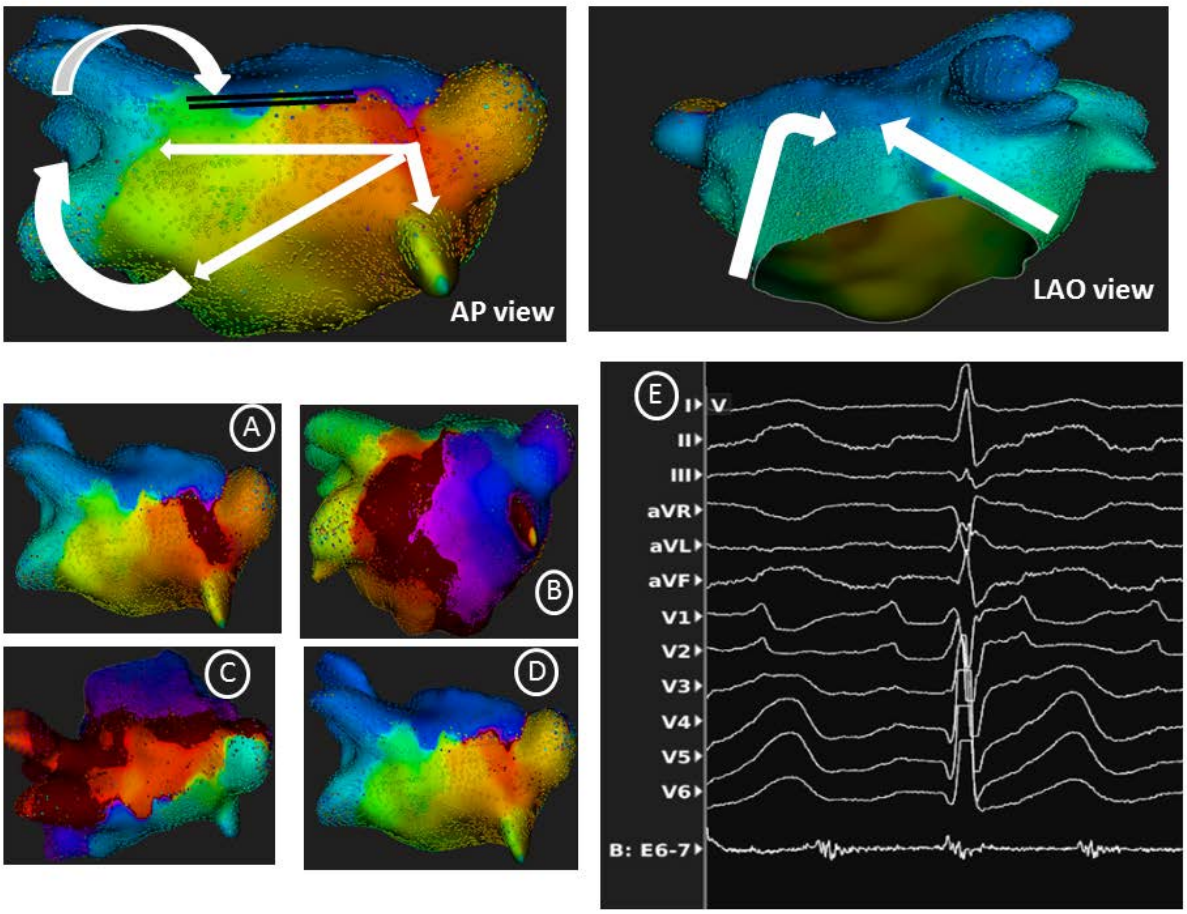

410

415

Figure 2.

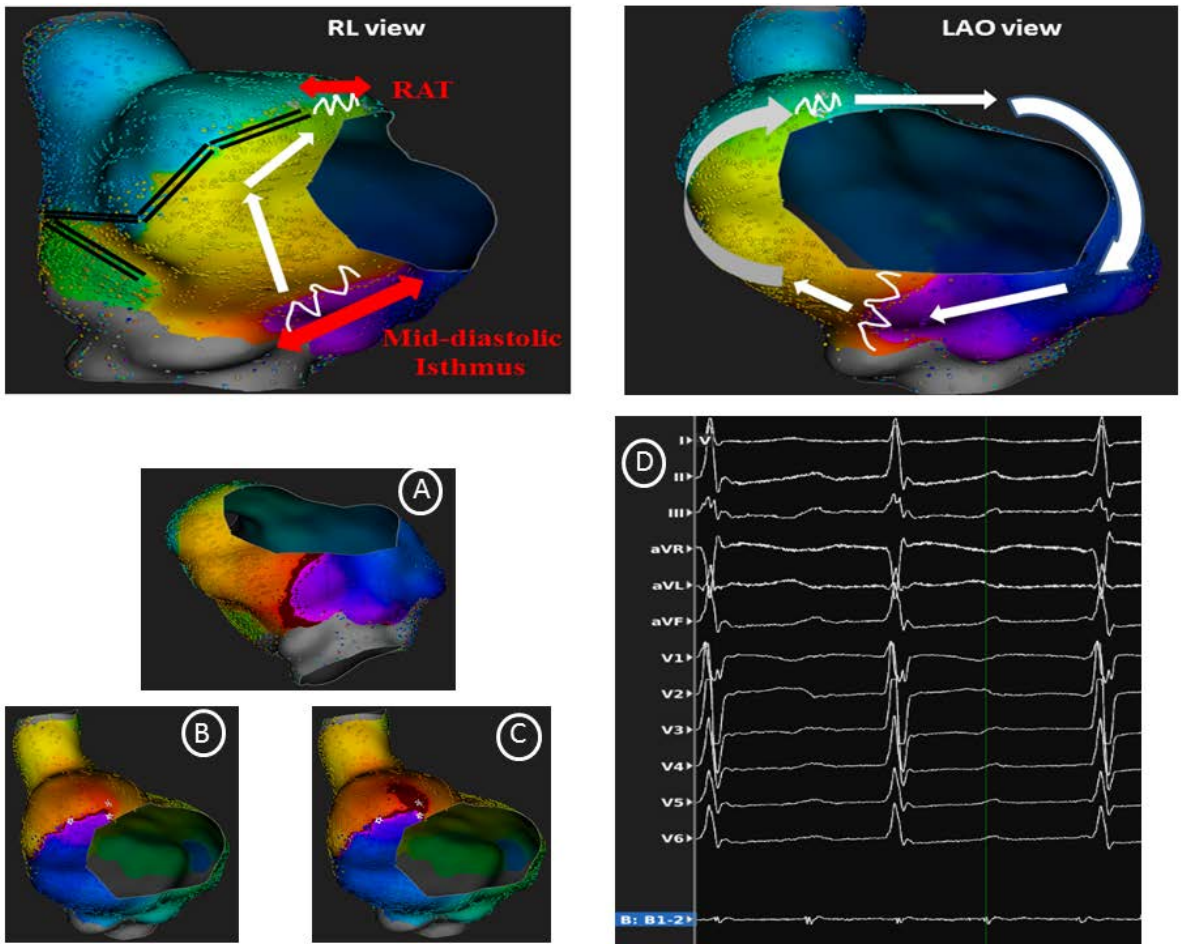

420

425

Figure 3.

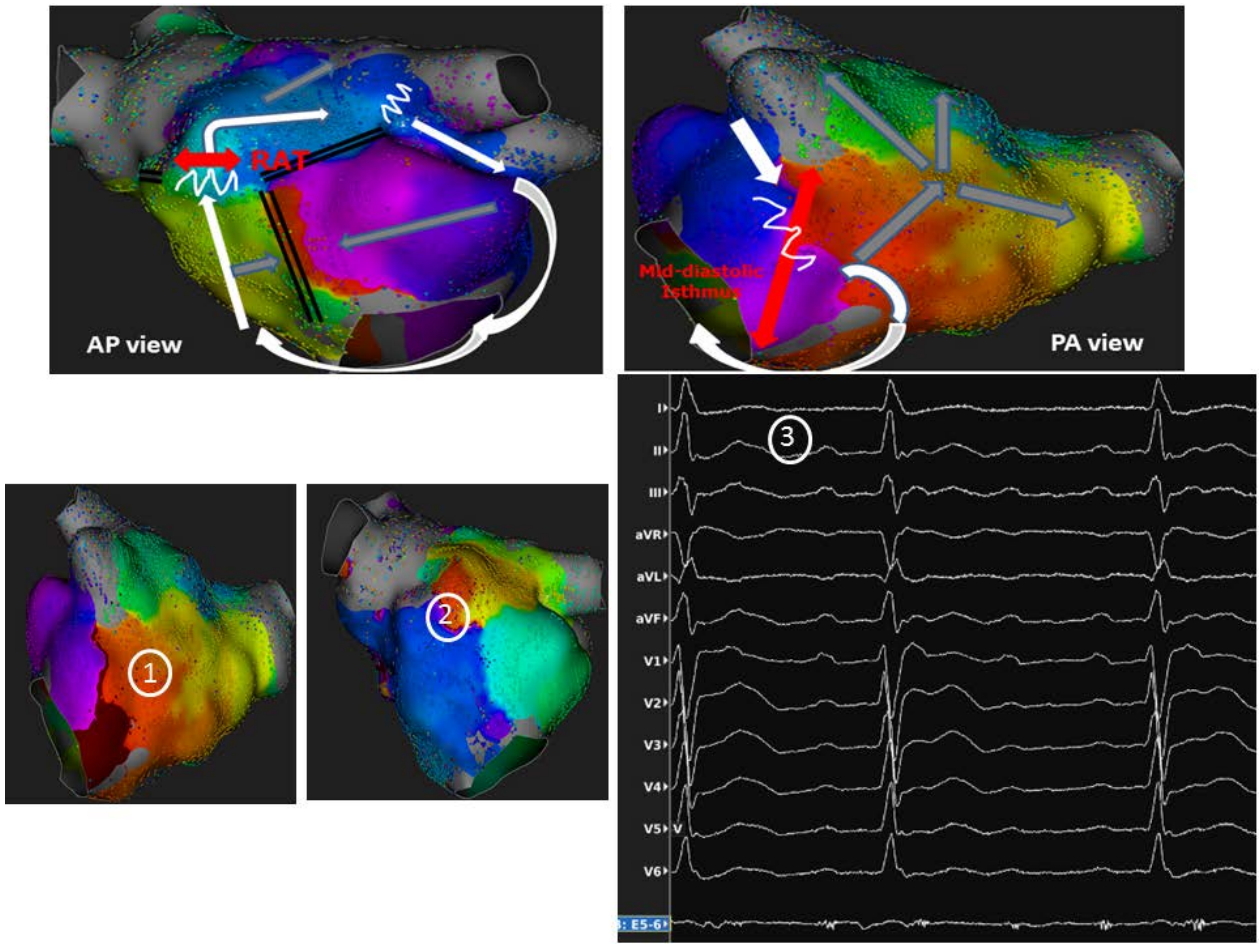
RAT
AP view
Mid-diastolic
Isthmus
PA view
1
2
3
I
II
III
aVR
aVL
aVF
V1
V2
V3
V4
V5
V6

Supplementary Figure 1

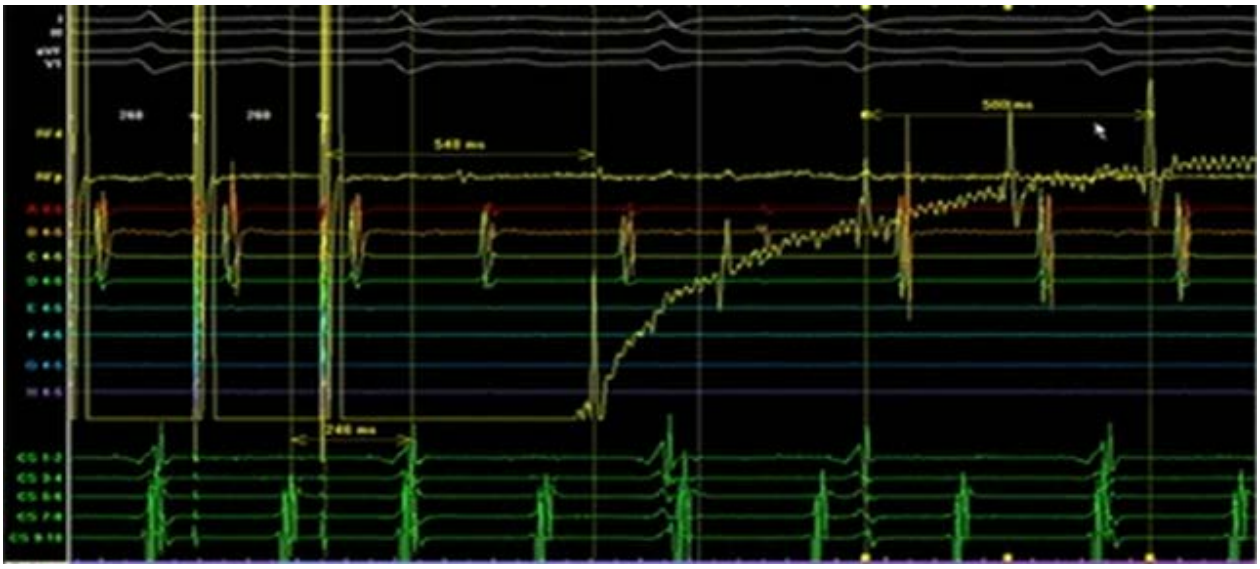

Supplementary Figure 2

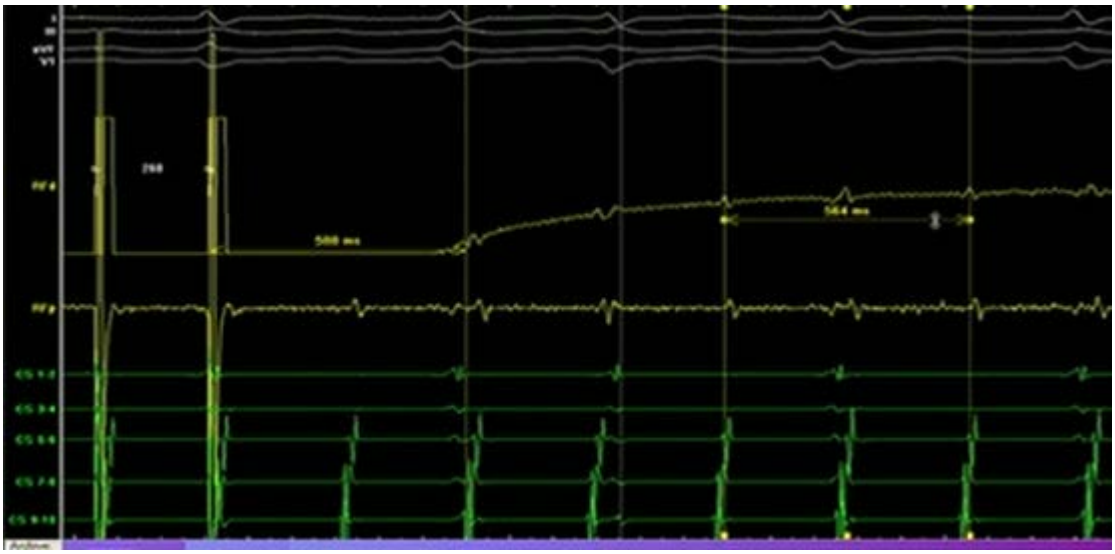

Supplementary Figure 3

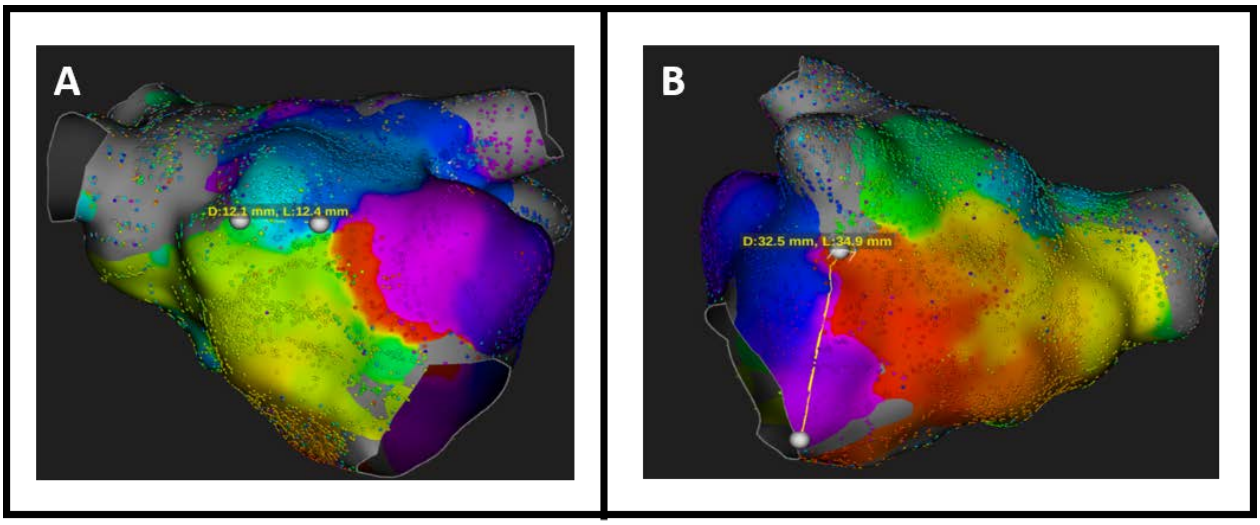

470